Transient Based Faulted Conductor Selection Method for Double Circuit Lines

J.S. Wijekoon, M.N. Haleem and A.D Rajapakse
University of Manitoba
Winnipeg, Canada
wiwmigjs@myumanitoba.ca, umnausha@myumanitoba.ca, Athula.Rajapakse@umanitoba.ca

***Abstract*-- A simple and fast method to identify the faulted conductors in a double circuit line with the help of a single circuit transient based fault type classifier is presented in this paper. In addition to a transient based single circuit fault type classifier, only currents locally measured through each conductor are required. Having known the fault type, the magnitudes of the rate of change of currents (ROCOC) through two circuits of faulted phases are compared by calculating three indices to find the conductors involved in the fault. The method can identify faulted conductors during both inter-circuit faults as well as intra-circuit faults. The method can be easily implemented on a simple hardware platform capable of performing filtering and simple mathematical functions. As only the current measurements in the frequency components between 0.5 kHz to 1 kHz are suggested, the need for high bandwidth current transducer is avoided.**

***Keywords*: Phase selection, faulted conductor identification, double-circuit line, fault classification.**

I. Introduction

Double circuit parallel transmission lines on the same tower are widely used due to advantages such as the narrow right of way [1], enhanced capacity, and improved reliability [2]. However, to assure critical reliability and stability requirements, it is required to minimize the degree of interruption of power flow between two-areas connected by such a high-capacity double circuit transmission line [3], [4] during faults. Prompt selective pole tripping, which requires a faulted conductor selection method for double circuit lines, can minimize the degree of interruption of power flow between the two areas [3] during line faults. Although not as widespread as in single circuit lines, the application of single-pole tripping in double circuit transmission lines is not uncommon [5], [6]. Therefore, a fast and accurate means of faulted conductor selection can contribute to enhancing the economic and reliability advantages of double circuit lines [2]. Faulted conductor selection in double circuit lines could be more imperative than faulted phase selection in single circuit lines due to more possible power transfer options and the higher impact on the system if both circuits happen to be taken out.

Mutual coupling and many possible fault types make double circuit line fault classification challenging [1], [7]. Different possible combinations of faults between the conductors in two parallel three-phase lines escalate to 120 fault types [1] when compared with the 11 possible fault types in a single circuit line [1] and making it harder to discriminate one type from another.

Power frequency-based faulted phase-detection schemes such as those presented in [7], [8] are commonly proposed for faulted phase selection in single circuit lines as well as double circuit lines. However, issues such as short critical clearing times and reduced short circuit currents due to high penetration of power electronics-based sources necessitate faster and more sensitive methods [4]. Typically, a relay employing phasor-based algorithms take around 1–1.5 cycles [9] to issue a trip signal, and after receiving a trip signal, an HV circuit breaker would take 2–3 cycles to interrupt the fault currents [9]. Hence the typical fault clearance times are in the range of 3–4.5 cycles, mainly restricted by the circuit breaker operating time. However, an opportunity exists to reduce the total interruption time by about 0.5-1 cycles by reducing the relay operating time.

Therefore, the application of transient based transmission line protection techniques is getting renewed attention due to challenges faced by the traditional phasor-based algorithms [10]. However, developing a transient based faulted conductor identification technique for a double circuit line is challenging [10]. This is because, in addition to the fault type itself, fault inception angle, fault location, and strong induced transients due to coupling among parallel conductors also influence the nature of the fault transients [7], [11]. Furthermore, identification must be completed in a sub-cycle period when used for protection applications [12].

Due to the complex nature of feature extraction, machine learning methods such as neural networks [13], [14] fuzzy logic [15], [16] etc., are often applied solitarily or as a combined fashion [17] for faulted conductor identification. Furthermore, the application of contemporary tools such as support vector machines (SVM), principle component analysis (PCA) based frameworks, genetic algorithm, etc. for faulted phase selection can be seen in recent literature [10]. However, the development of customized fault classifiers using such techniques is a very complicated and time-consuming task as they demand the generation of large sets of training data and involve a lengthy process of training [13], [14]. For example, in [11] more than 2400 data sets were used for the training of neural networks and in [18] approximately 30000 data sets were used for training. Therefore, such methods come with a high engineering cost and the trained machine learning models may require retraining, if

J.S. Wijekoon, M.N. Haleem and A.D. Rajapakse are with the Department of Electrical and Computer Engineering, University of Manitoba, Winnipeg, MB R3T 5V6, Canada. (email:wiwmigjs@myumanitoba.ca,umnausha@myumanitoba.ca,athula.rajapakse@umanitoba.ca)

the system topology changes substantially. Furthermore, finding suitable hardware to implement some of the above techniques may be challenging.

In this paper, a comprehensive approach to identify the conductors involved in a fault by comparing the observed maximum rates of change of locally measured currents in the conductors is presented. This method is a further development of the approach proposed in [19] to find the faulted phase(s) of a single-circuit transmission line by comparing the maximum rate of change of current (ROCOC) of each phase against the others. The novel features that distinguish the current paper from the previous proposal in [19] are the new capabilities: namely the applicability to double circuit lines and ability to categorize inter-circuit faults unlike the methods in [11], [18], [15], [16] which are restricted to classify only intra-circuit fault scenarios. The key to discriminate inter-circuit faults is a new index calculated from the currents of two conductors of the same phase. Upon detecting the phase(s) involved in the fault with a method such as [19], conductor(s) involved in the fault is identified with the help of indices associated with the faulted phase(s).

Since the proposed method does not rely on voltage measurements, the proposed method avoids the need for specially designed transducers for voltage measurements as in [3]. The proposed method relies on single-ended measurements and avoids the need for a communication channel for transmitting the remote terminal measurements. When compared with the adaptive cumulative sum based method proposed in [12], [20] that need 3 ms data window, the method can identify the faulted conductors with the help of only 1 ms measurement window and avoids the need for calculating phasors of the current measurements. The implementation of the proposed algorithm does not involve a laborious training phase as in [7], [18], [11], and [15], much easier to implement as the indices are almost independent of fault resistance, and need only simple hardware due to the simplicity of the algorithm. Despite its simplicity, the proposed faulted conductor identification method is robust and accurate.

II. Faulted Conductor(s) Identification By Comparing Rate of Change of Currents

Faulted conductor(s) in a three-phase AC transmission line cannot be determined straightforwardly just by considering the strength of the observed transient as it varies with the fault location, fault resistance, fault inception angle, and mutual coupling between the conductors. A fault in one conductor of a closely coupled transmission line induces strong transients in the other conductors. However, the pairwise comparison of ROCOC greatly reduces the complexity of faulted phase selection [19]. In this paper, the pairwise comparison approach in [19] is extended to identify the faulted conductor(s) in a double circuit transmission line, as schematically shown in Fig. 1.

Changes in the current through the faulted conductor(s) induce changes in voltage in the healthy conductors and the change in voltage across the mutual capacitance injects current to the healthy conductor. Therefore, a fault in one/two-conductor(s) may cause strong transients in the healthy conductors, which are dependent on the strength of the transient in the faulted conductor and the mutual coupling between the conductors.

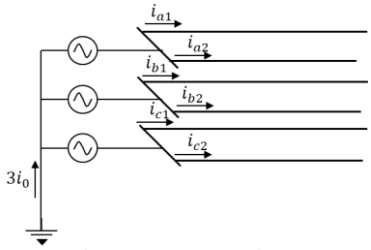

Fig. 1. Currents caused by a fault in one circuit of double circuit line

Therefore, if the strength of the faulted transients is compared, the likely source of the transient can be identified. This paper proposes the index F_{p1_p2} defined in (1) to identify the faulted conductor(s) among the coupled conductor pair p_1 and p_2.

$$F_{p1\_p2} = \frac{\max\left(\left|\frac{di`_{p1}}{dt}\right|\right) - \max\left(\left|\frac{di`_{p2}}{dt}\right|\right)}{\max\left(\left|\frac{di`_{p2}}{dt}\right|\right)} \quad (1)$$

where $i`_{p1}$ and $i`_{p2}$ are bandpass filtered instantaneous currents i_{p1} and i_{p2} in the conductors p_1 and p_2. The index is defined considering the peak rate of change of conditioned current observed within a short time window after a fault. The signal conditioning involves fault detection and band-pass filtering, which will be explained in Section III. If only conductor p_1 is involved in a fault, F_{p1_p2} is greater than zero. Similarly, if only conductor p_2 is involved in a fault, F_{p1_p2} is less than zero. If F_{p1_p2} is close to zero then either both conductors are involved in the fault or both conductors are not involved in the fault

III. Algorithm For Faulted Conductor Identification for Double Circuit Lines

This section describes the proposed faulted conductor selection logic developed using the index proposed in the previous section and the signal processing associated with the extraction of the rate of change of current signals. Before explaining the proposed faulted conductor selection method, a brief description of the faulted phase selection algorithm proposed in [19] which is the first stage of the proposed algorithm is included in this section for the sake of completeness.

A. Faulted Phase Selection Method

An index to identify the faulted phases using the pairwise comparison approach has been defined in [19]. The proposed index is given in (2).

$$F_{pq} = \frac{\max\left|{di_p(t)}/{dt}\right|}{\max\left|{di_q(t)}/{dt}\right|} \quad (2)$$

where $i`_p$ and $i`_q$ are bandpass filtered instantaneous currents i_p and i_q in the phases P and Q. The proposed index measures the relative strength of the fault generated transient in one phase to the fault generated transient in another phase. Similar to (1), the index is defined considering the peak rate of

change of conditioned current observed within a short time window (1 ms) after a fault. Based on the value of the index, the following three conclusions can be made.

1) If $F_{pq} \approx 1$, then both phases P and Q are involved in the fault or not involved in the fault.
2) If $F_{pq} \gg 1$, then phase P is involved in the fault and phase q is not involved in the fault
3) If $F_{pq} \ll 1$, then phase P is not involved in the fault and phase Q is involved in the fault.

Three indices are defined as F_{ab}, F_{bc}, F_{ca}, using (2) in [19]. Based on the three indices, a complete solution for faulted phase selection algorithm for single circuit lines has been developed. Three indices and the instantaneous residual current are calculated continuously until detecting a fault. Upon detecting a fault, the values of each index are compared after the time window as depicted in Fig. 2. The ground faults are discriminated from the phase-to-phase and three-phase faults using the residual current ($3i_0$) as a ground fault causes a large residual current and it is ideally zero during a phase-to-phase or three-phase faults. Upon discriminating the ground faults from ungrounded faults, the values of the three indices are compared to identify the faulted phases. The conditions behind identifying the faulted phases are summarized below. More information about the logic behind forming those conditions can be found in [19].

1) Phase Selection Conditions for Phase-to-Phase Faults

For a Phase-P-to-Phase-Q fault, the following three criteria must be satisfied [19].

$$(1 - \epsilon_2) \le F_{pq} \le (1 + \epsilon_3) \quad (3)$$

$$(1 + \epsilon_4) \le F_{pr} \quad (4)$$

$$(1 - \epsilon_5) \ge F_{rp} \quad (5)$$

where R is the heathy phase, and $\epsilon_1 - \epsilon_5$ are positive tolerance settings.

Any ungrounded fault that does not satisfy (3), (4), and (5) are categorized as three-phase faults.

2) Phase Selection Conditions for Phase-to-Ground Faults

Upon discriminating a ground fault using the presence of residual current, the faulted phase in a Phase-P-to-Ground fault can be identified using the conditions (6), (7), and (8) [18].

$$(1 - \epsilon_6) \le F_{qr} \le (1 + \epsilon_7) \quad (6)$$

$$(1 + \epsilon_8) \le F_{pq} \quad (7)$$

$$(1 - \epsilon_9) \ge F_{rp} \quad (8)$$

where Q and R, are healthy phases, and $\epsilon_6 - \epsilon_9$ are positive tolerance settings.

3) Phase Selection Conditions for Phase-to-Phase-to-Ground Faults

A phase-to-phase-to-ground fault is identified by the presence of residual current and failure to satisfy the criteria (6) – (8). Upon identifying a phase-to-phase-to-ground fault, the phase involved in the fault is identified by the index having a greater magnitude. As an example, if F_{pq} is the largest index, Phase-P is involved in the fault. Then, the index corresponding to two other phases, F_{qr}, is compared to identify the remaining phase involved in the fault. If F_{qr} is greater than unity, Phase-Q is involved in the fault; otherwise, Phase-R is involved in the fault [19].

The same faulted phase selection algorithm can be applied to double circuit lines by replacing each phase current with the sum of two currents through the two circuits belonging to the same phase. That is $i`_a = i`_{a1} + i`_{a2}$ ; $i`_b = i`_{b1} + i`_{b2}$; and $i`_c = i`_{c1} + i`_{c2}$. This procedure enables the identification of phases involved in a fault, as described in Fig. 2.

B. Faulted Conductor Selection Logic

The second stage involves the identification of the conductors involved in the fault, including those involving inter-circuit faults on the double circuit line. This can be achieved by comparing the maximum ROCOC values of the pair of conductors belonging to the same phase. Three indices, F_{a1_a2}, F_{b1_b2}, F_{c1_c2}, can be defined to compare the maximum ROCOC values of the pair of conductors belonging to each phase using (1). If the index is close to zero, it could mean either that (i) both conductors are involved in the fault or (ii) both are not involved in the fault. For example:

1) During an inter-circuit phase-to-phase fault where Phase-C of circuit-1 and Phase-B of circuit-2 is involved, $F_{b1\_b2} < 0$ and $F_{c1\_c2} > 0$ since the maximum ROCOC of Phase-B of circuit-2 and Phase-C of circuit-1 is greater than the maximum ROCOC of Phase-B of circuit-1 and Phase-C of circuit-2 respectively. Moreover, $F_{a1\_a2} \approx 0$ since phase-A is not involved in the fault.
2) Similarly, during an intra-circuit phase-A-to-phase-B fault in circuit-1, $F_{a1\_a2} > 0$ and $F_{b1\_b2} > 0$ since the maximum ROCOC of phases A and B of circuit-1 is greater than their counterparts in circuit-2. Furthermore, $F_{c1\_c2} \approx 0$ since Phase-C is not involved in the fault.

Therefore, having determined the fault type in the first stage, conductors involved in the fault can be identified with the help of three indices comparing inter circuit currents, as detailed in the following subsections.

1) Faulted Conductor Identification in Phase-to-Ground Faults

The logic for identifying the faulted conductor involved in a phase-to-ground fault is explained using a Phase-A-to-ground fault. If the faulted phase selection algorithm detects a Phase-A-to-ground fault, the faulted conductor selection algorithm would check the value of the F_{a1_a2} index to identify the faulted conductor.

Hence the faulted conductor involved in the Phase-A-to-ground fault can be identified using the logic in (9).

$$\begin{aligned} &if\ \{F_{a1\_a2} > 0\}\text{: Phase} - \text{A in Circuit} - 1 \\ &else\ if\ \{F_{a1\_a2} < 0\}\text{: Phase} - \text{A in Circuit} - 2 \end{aligned} \quad (9)$$

Therefore, using (10), the faulted conductor involved in any phase-to-ground fault can be identified.

$$\begin{aligned} &if\ \{F_{p1\_p2} > 0\}\text{: Phase} - \text{P in Circuit} - 1 \\ &else\ if\ \{F_{p1\_p2} < 0\}\text{: Phase} - \text{P in Circuit} - 2 \\ &\text{where } p \in A, B, C \end{aligned} \quad (10)$$

2) Faulted Conductors Identification in Phase-to-Phase and Phase-to-Phase-to-Ground Faults

Consider a Phase-A-to-B fault detected by the phase selection algorithm. Then the faulted conductor selection algorithm check F_{a1_a2} and F_{b1_b2} indices.

The faulted conductors can be identified using the logic in (11)

$$\begin{aligned} &if\ \{F_{a1\_a2} > 0\ \&\ F_{b1\_b2} > 0\}\text{:} \\ &\quad \text{Phases A \& B in Circuit} - 1 \\ &else\ if\ \{F_{a1\_a2} < 0\ \&\ F_{b1\_b2} > 0\}\text{:} \\ &\quad \text{Phase A in Circuit} - 2\ \&\ \text{Phase B in Circuit} - 1 \end{aligned} \quad (11)$$

else if $\{F_{a1\_a2} > 0 \;\&\; F_{b1\_b2} < 0\}$:
Phase A in Circuit − 1 & Phase B in Circuit − 2
else if $\{F_{a1\_a2} < 0 \;\&\; F_{b1\_b2} < 0\}$:
Phases A & B in Circuit − 2

Thus using the generalized logic in (12), the faulted conductors involved in any phase-to-phase or any phase-to-phase-to-ground fault can be identified.

if $\{F_{p1\_p2} > 0 \;\&\; F_{q1\_q2} > 0\}$:
Phases p & q in Circuit − 1
else if $\{F_{p1\_p2} < 0 \;\&\; F_{q1\_q2} > 0\}$:
Phase P in Circuit − 2 & Phase Q in Circuit − 1
else if $\{F_{p1\_p2} > 0 \;\&\; F_{q1\_q2} < 0\}$: (12)
*P*hase P in Circuit − 1 & Phase Q in Circuit − 2
else if $\{F_{p1\_p2} < 0 \;\&\; F_{q1\_q2} < 0\}$:
Phases P & Q in Circuit − 2
where: $P, Q \in \{A, B, C\}$

3) Faulted Conductors Identification in Three-Phase Faults

Conductor identification in three-phase faults follows the same logic presented in previous subsections. The only difference is the conductor selection algorithm will consider the value of all three indices and decide the faulted conductor based on whether each index is greater than or less than 0. If all three indices are greater than 0 then all three conductors in circuit-1 are involved in the fault. If all three indices are less than 0 then all three conductors in circuit-2 are involved in the fault. Any other combination will represent an inter-circuit fault. The faulted conductors involved in the inter-circuit fault can be identified by checking the sign of each index.

The algorithm to identify the faulted conductors is shown in Fig. 3. All indices are continuously calculated considering a fixed-length sliding window, however, the faulted conductor identification logic is triggered only after confirming the presence of a fault. As depicted in Fig. 3, the method is capable of identifying conductors involved in inter-circuit faults, which are shown in pink color, as well as intra-circuit faults, shown in green and blue color. If the approach proposed in [19] is directly applied to a double circuit transmission line, it would require 15 indices and 15 thresholds to cover all the conductor combinations in a double circuit transmission line susceptible to cross circuit faults. The new approach proposed in this paper requires only three additional indices to handle all possible fault types, greatly simplifying the algorithm. Also, there is some rare possibility of occurring faults involving more than three conductors. Identification of faulted conductors in such faults is not considered in this paper, as single-pole tripping or quick recovering from such severe faults is practically difficult.

C. Signal Processing

Fig. 4 shows the signal processing involved in calculating indices for the proposed conductor selection algorithm. Fig. 4 (a) depicts the max *di/dt* calculation stage of the signal processing block. The instantaneous current signals are bandpass filtered to remove the influence of the power frequency component and the high-frequency noise. The lower cut-off frequency of the bandpass filter minimizes the impact of power frequency and harmonics while the upper cut-off frequency is set to minimize the influence of induced transients from other phases in calculating max (*di/dt*) values. Then the ROCOC of the bandpass filtered current is calculated using the derivative function. The absolute value of the ROCOC is passed to the maximum detecting function through a control switch. When the control input Sp is set to 0, the absolute ROCOC values are passed to the maximum detector function. Fig. 4 (b) depicts the fault detection and index calculation stage of the signal processing block. Fault detection is achieved by comparing the sum of peak *di/dt* values against a threshold. Once a fault is detected, the comparator sends a signal to the control switch connected to the output of the index calculation block. The same signal is delayed and fed back to the maximum detection block depicted in Fig. 4 (a). The maximum values of signal *di/dt* are tracked for a period of T_D and made available for computing the index after the time delay T_D.

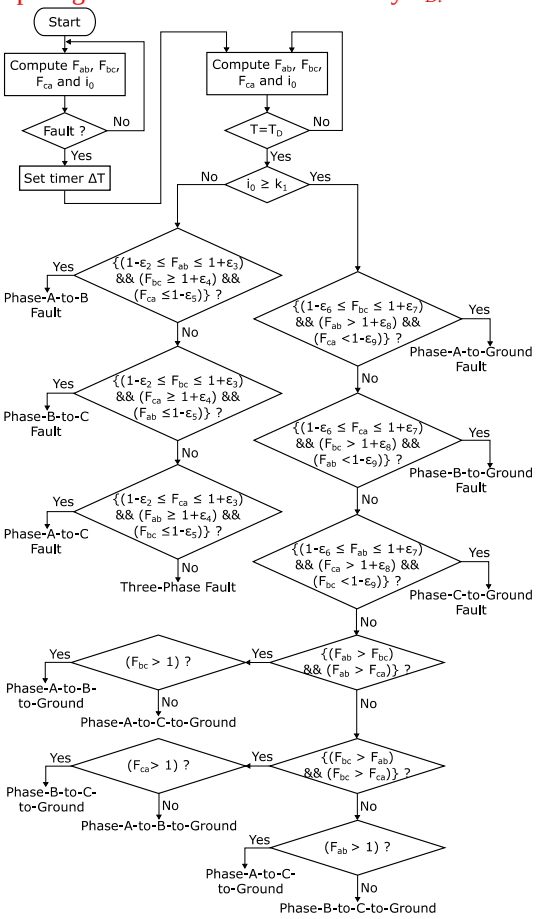

Fig. 2 Single Circuit Transient Based Fault Classifier (Stage 1) [19]

IV. Test System

The algorithm was verified by applying it to the 230 kV transmission system shown in Fig. 5. The power system was simulated in PSCAD/EMTDC™ electromagnetic transient simulation software with 10 µs time steps. The design of the 150 km long overhead transmission line is shown in Fig. 6. The transmission lines were modeled as ideally transposed frequency-dependent phase models. Chukar conductors having a DC resistance of 0.0203 Ω/km and a radius of 0.032m were used for phase conductors. The DC resistance and radius of ground conductors are 2.8645 Ω/km and a radius of 0.0055m, respectively. A ground resistivity of 100 Ωm was assumed. The current transformers are modeled using the Lucas model available in the protection library in PSCAD/EMTDC™ simulation software with a ratio of 400:1. The three-phase

transformer data are provided in Table I. The faults were modeled as two-state resistances (1 MΩ no-fault, 0.01Ω short circuit).

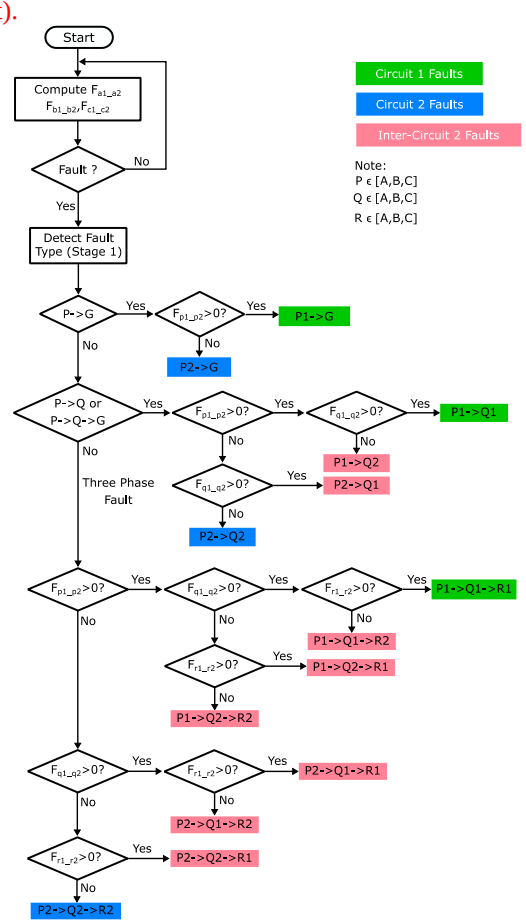

Fig. 3 Proposed Faulted Conductor(s) Identification Algorithm for Double Circuit Transmission Lines

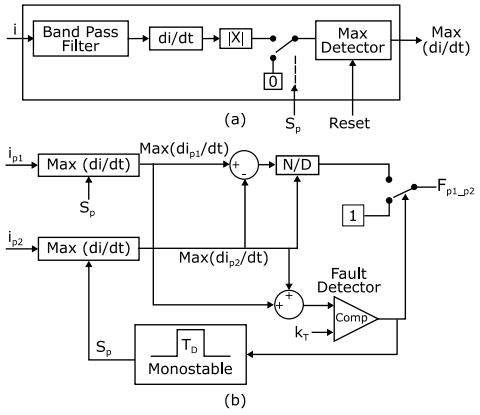

Fig. 4 Calculating The Faulted Conductor Identification Indices (a) Max(*di/dt*) Detector, (b) Index Calculation

The parameters of the signal processing scheme shown in Fig. 4 were determined through a systematic simulation study similar to the one described in [21]. Based on these studies, the lower cut-off frequency of the band-pass filter was set to 0.5 kHz and the upper cut-off frequency was set to 1 kHz. The fault detection threshold k_T, which should be set above the sum of peak di/dt values observed under normal operation, was set to 1 kA/s. The length of the time window used for determining peak ROCOC values, T_D , was set to 0.2 ms for the conductor selection stage where as for phase selection stage it is set to 1ms [19]. These parameters can be fine-tuned to a given system, but the selected parameters are applicable for a wide range of line lengths and signal sampling rates as will be demonstrated.

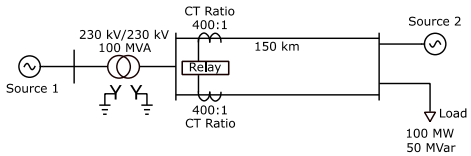

Fig. 5 The Test System with a 230 kV Double Circuit Transmission Line

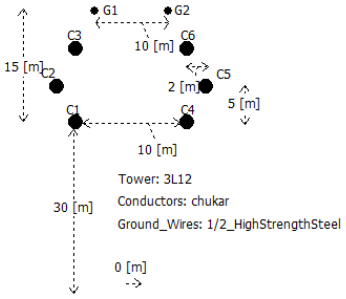

Fig. 6 Design of Overhead Double Circuit Transmission Line

TABLE I
TRANSFORMER DATA

Parameter	Value
Winding-1 Line-to-Line Voltage (RMS)	230 kV
Winding-2 Line-to-Line Voltage (RMS)	230 kV
Transformer MVA	100
Positive Sequence Leakage Reactance	0.1 p.u
Air Core Reactance	0.2 p.u
Magnetizing Current	2.0 %
Knee Voltage	1.25 p.u

V. RESULTS

A. Demonstration of Basic Algorithm and Challenges

Since the fault type identification part of the algorithm has been validated in [19], the results are focused on demonstrating the identification of the faulted conductors in inter-circuit faults. Fig.7 shows the instantaneous phase current signals in circuits-1 and 2 (Fig. 7(a), Fig. 7(b) and Fig. 7(c)) and their band passed versions (Fig. 7(d), Fig. 7(e) and Fig. 7(f)) for an inter-circuit phase-to-phase fault with a fault resistance of 75 Ω at 50 % of line length where Phase-A of circuit-1 and Phase-B of circuit-2 is involved. The change in Phase-A current in circuits 1 and 2 is almost the same even though there is a significant difference in Phase-B current in circuits 1 and 2 while Phase-C currents remain the same. This would lead to an incorrect faulted phase identification decision if a simple current magnitude comparison based faulted phase identification scheme was used since the difference between Phase-A currents is insignificant. However, the band-pass filtered versions of the same current signals (Figs. 7(d), (e) and (f)) depict significant transients in the faulted phases in circuit 1 and 2 while the transients in Phase-C currents are identical since Phase-C is not involved in the fault. This helps to identify the faulted phases correctly. This signifies the need for a transient based faulted phase identification scheme since a simple magnitude comparison based faulted phase identification scheme would not work in high resistance fault scenarios as depicted in Fig. 7.

Fig.8 shows the F_{p1_p2} ratios calculated for the above fault scenario. From the figure, it is clear that indices $F_{a1\_a2} > 0$, $F_{b1\_b2} < 0$ and $F_{c1\_c2} \approx 0$ and therefore, according to (1)

and the prior knowledge of fault type, faulted phases involved in this fault are identified as Phase-A of circuit 1 and Phase-B of circuit 2. Fig. 8 shows the values of the three ratios during the fault.

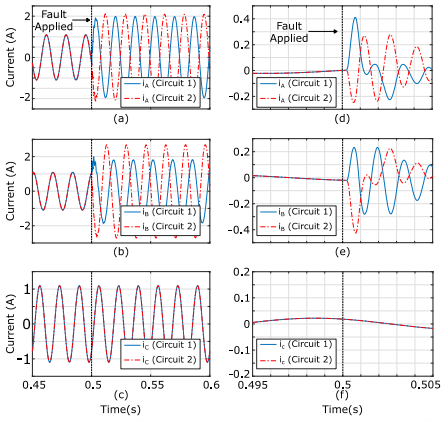

Fig. 7 Conductor Currents for a Fault Between, Phase-A of Circuit-1, and Phase-B in Circuit-2 (a), (b) and (c) Before and (d), (e) and (f) After Band-Pass Filtering

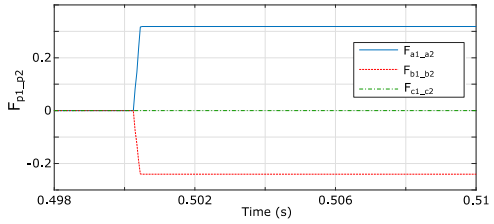

Fig. 8 F_{p1_p2} Ratios Calculated for A1-B2 Inter-Circuit Fault

Fig. 9 shows the calculated ROCOC values for a Phase-B to ground fault on circuit-1 at 95% of the line. The fault inception angle is 0 degrees in Fig. 9(a) whereas it is 90 degrees in Fig. 9(b). The maximum ROCOC value of the faulted conductor (Phase-B of circuit-1) shown in Fig. 9(b) is 9.85 kA/s for the metallic fault when the fault inception angle is 90 degrees. However, when the fault inception angle is 0 degrees at the same location for a metallic fault, the maximum ROCOC value of the faulted conductor is 1.282 kA/s. Therefore, the faulted conductor cannot be found with a simple magnitude comparison of ROCOC values. Furthermore, as depicted in Fig. 9, the ROCOC value changes with the fault resistance. Moreover, as depicted in Fig. 9(a) and Fig. 9(b) the ROCOC values significantly change with the fault inception angle.

Since there is no apparent simple relationship between the observed transient magnitudes and the conductors involved in the fault, it is not straightforward to solve the faulted conductor identification problem. However, the proposed indices and systematic logic can overcome the difficulties and accurately determine the conductors involved in faults.

To examine the effect of transmission line length on the transient signals considered for calculating the fault indices, a 300 km double circuit line is compared with the 150 km double circuit line. Fig. 10 shows the variations of ROCOC of Phase-A current in Circuit-1 and Circuit-2 for a Phase-A-to-Ground fault applied in Circuit-1 at 5 % of line length. The variations of the ROCOC when the transmission line length is increased up to 300 km are also plotted on the same figure. Fig. 11 shows the variations of ROCOC of Phase-A current when the fault is applied at 95 % of line length. The variation of ROCOC for 150 km long transmission line and 300 km long transmission line is similar within the time window considered for computing fault indices, irrespective of the fault location, even though the current waves of the 300 km line arrive later than that of the 150 km line. Since the fault indices are computed as the ratios of the peak di/dt values, they remain more or less the same for both 150 km and 300 km lines. Therefore, the algorithm's performance is not affected by the length of the transmission line. Further simulation experiments, results of which are not shown due to lack of space, showed that ground resistivity has no significant impact on the performance, and the observed signals are similar for both transposed and untransposed lines.

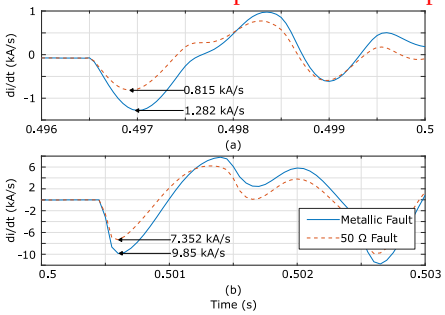

Fig. 9 Calculated ROCOC Values for a Metallic and 50Ω Phase-B1-to-Ground Fault at 95 % of the Length from the Relay (a) at θ_A=0, (b) θ_A=90

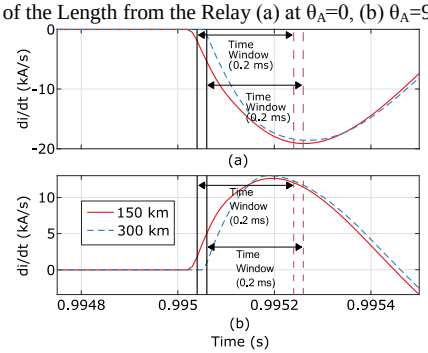

Fig. 10 Rate of Change of Phase-A Current in (a) Circuit-1 and (b) Circuit-2 for a Phase-A-to-Ground fault in Circuit-1 at 5% of the length. Two curves are for 150 km and 300 km lines.

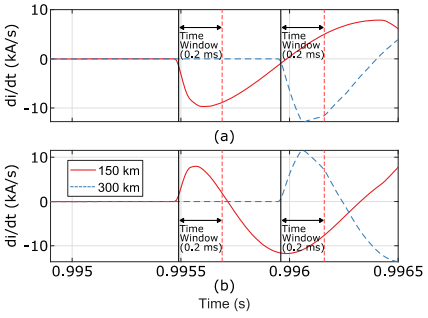

Fig. 11 Rate of Change of Phase-A Current in (a) Circuit-1 and (b) Circuit-2 for a Phase-A-to-Ground fault in Circuit-1 at 95 % of length. Two curves are for 150 km and 300 km lines.

In this study, it is assumed that fault type is correctly determined using the procedure in Fig. 2 (as validated in [19]) and therefore, the results presented in the next few sections are focused on the determination of the conductors involved in inter-and intra-circuit faults.

B. Identification of Faulted Conductor for Phase-to-Ground Faults

Fig. 12 (a) and (b) show the calculated Phase-A index, F_{a1_a2}, for circuit-1 Phase-A-to-ground faults and circuit-2 Phase-A-to-ground faults respectively for three fault resistance values

(0.1Ω, 5Ω, 50Ω). The values of the index were computed for every 3 degrees of the fault inception angles. Although the calculated index changes with the fault inception angle for a given fault location, the index is almost independent of the fault resistance. According to Fig. 12, regardless of the fault resistance and fault inception angle, the criterion presented in Fig. 3 is satisfied except for a short window of 6 degrees where F_{a1_a2} <0 when F_{a1_a2} >0 is expected and vice versa. For both the cases presented, the faulted conductor is correctly identified for all other fault inception angles.

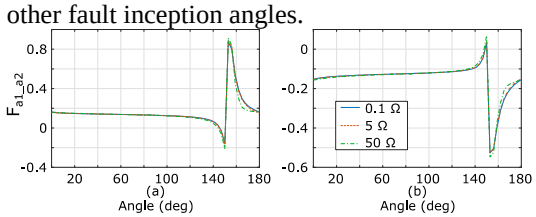

Fig. 12 Fault indices for Phase-A-to-ground faults at 90 % (a) Conductor-A1-to-ground, (b) Conductor-A2-to-ground

The influence of the fault location in faulted conductor classification is evaluated by applying faults between 15 % of the line length to 95 % at 9 regular locations. Fig. 13(a) shows the calculated index F_{b1_b2} for circuit-2 Phase-B-to-ground metallic faults. Fig. 13(b) shows the same index for 50 Ω faults. Faults were applied in 1-degree increments of fault inception angle. For all the cases presented, the faulted conductor is correctly identified except during a short window of fault inception angles.

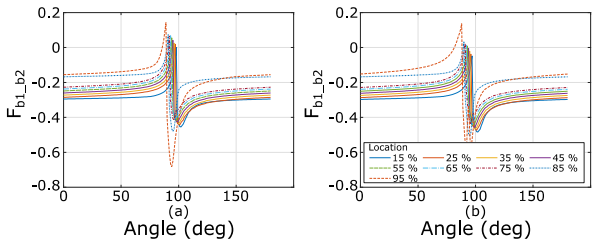

Fig. 13 Calculated fault index F_{b1_b2} for circuit-2 Phase-B-to-ground faults along the line (a) Metallic faults, (b) 50 Ω faults.

The window of fault inception angles where the algorithm fails to identify the faulted conductors coincide with the voltage zero crossing of the faulted phase. When the fault occurs near the voltage zero crossing, the strength of the induced transients in the non-faulted phases becomes larger than the strength of the transient in the faulted phase. This reduces the sensitivity of the algorithm for faults happening around the voltage zero crossings.

C. Identification of Faulted Conductors for Phase-to-Phase Faults

Subcategories of faults that are involved in this class of faults are Intra/inter circuit line-to-line faults and intra/inter line-to-line-ground faults. Fig. 14 demonstrates the identification of faulted conductors during a line-to-line (Phase-A-to-Phase C) fault within the circuit and between circuits.

Having determined that a Phase-A-to-Phase-C fault has occurred, the signs of indices F_{a1_a2} and F_{c1_c2} are tested. As depicted in Fig. 14(a) and Fig. 14(c), both positive indices reflect an intra-circuit fault within circuit-1. However, as depicted in Fig. 14(d) and Fig. 14(f), opposite signs of respective indices, F_{a1_a2} and F_{c1_c2}, reflect an inter-circuit fault. The negative value of F_{a1_a2} in Fig. 14(d) indicates the involvement of Phase-A in circuit-2 and the positive values of F_{c1_c2} shows the involvement of Phase-C in circuit-1 in the fault.

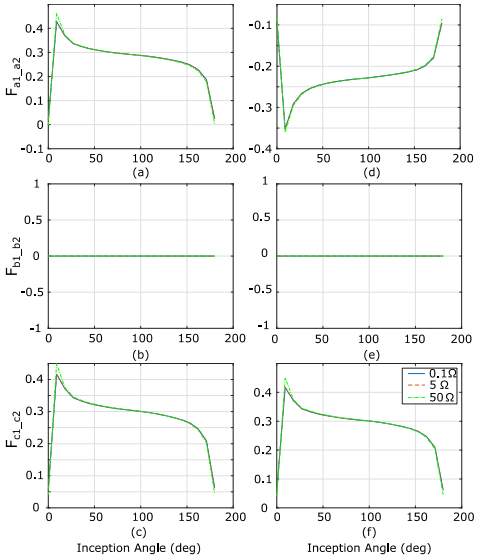

Fig. 14 Inter-circuit faults and intra-circuit faults at 50 % line length (a) - (c) Intra-circuit fault A1-C1, (d) - (f) Inter-circuit fault A2-C1

D. Identification of Faulted Conductors for Three-Phase Faults

Once a three-phase fault is detected, signs of all three indices are tested to find conductors in each circuit is involved in the fault. For example, the positive sign of F_{a1_a2} and negative signs of indices F_{b1_b2} and F_{c1_c2} reflect the involvement of the following conductors, Phase-A in circuit-1, Phase-B in circuit-2, and Phase-C in circuit-2 in the fault considered in Fig. 15(a)-(c). Similarly, it can be recognized that the three-phase fault corresponding to Fig. 15(d)-(f) involves Phase-A in circuit-2, Phase-B in circuit-1, and Phase-C in circuit-2.

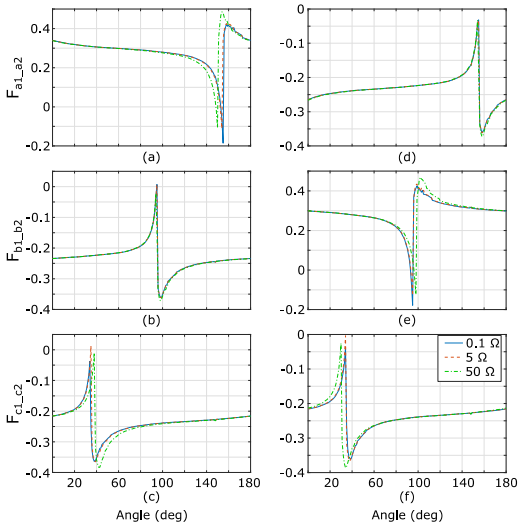

Fig. 15 Inter-circuit three-phase faults at 90 % line length (a) - (c) A1-B2-C2, (d) - (f) A2-B1-C2

However, as depicted in Fig. 15(a), for a short window of about 6 degrees of the fault inception angle, the algorithm wrongly declares as the conductor A2 is involved in the fault. Similarly, for an intra-circuit three-phase fault in circuit-1, as depicted in Fig. 16(a) for a short window of 6 degrees the algorithm incorrectly declares that the fault is an inter-circuit fault where conductor A2 is involved in the fault instead of

conductor A1.

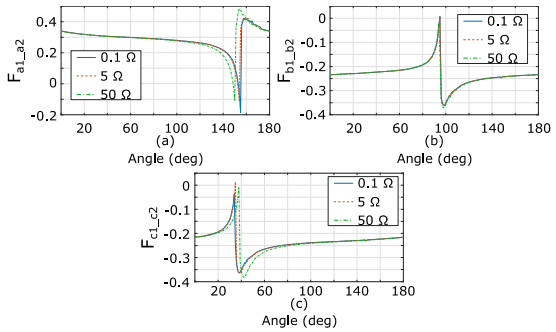

Fig. 16 Metallic three-phase fault in the middle of circuit-1 (a) F_{a1_a2}, (b) F_{b1_b2}, and (c) F_{c1_c2}

The sensitivity of the proposed algorithm is reduced for faults involving more than one phase when the faults occur around fault inception angles where the pre-fault voltage difference between the faulted phases is close to zero. This will lead to incorrect faulted conductor identification decisions.

The effect of sampling rate on the accuracy of the proposed algorithm was also analyzed in the validation process. The analysis revealed that a low-cost signal sensing and pre-processing hardware solution can be used since the method work even at lower sampling rate such as 10 kHz and the required minimum bit resolution of the ADC is only 8 bits.

VI. Conclusions

A simple method of utilizing a set of indices determined using the peak rate of change of the currents in conductors immediately after a fault is proposed for identifying the fault type and the faulted conductors in a double circuit line. The results show that the method is not significantly affected by the fault resistance and the fault location, and it is applicable for both transposed and untransposed lines of a wide range of line lengths. The proposed faulted conductor identification method is much faster than phasor based algorithm since the total decision making time, which is constrained by the time window used for the faulted phase selection part of the algorithm, is slightly over 1 ms. The simulation-based verification showed that the method is very accurate in identifying conductor(s) involved in a fault during phase-to-ground faults and phase-to-phase faults. However, the sensitivity of the method is reduced for a short window of fault inception angles around the voltage zero crossings, which is a common limitation observed in transient based methods.

VII. References

[1] W. Q. Jiang, Q. J. Liu and C. J. Li, "Review of fault location for double-circuit parallel transmission lines on the same pole," in *2011 Int. Conf. on Advanced Power System Automation and Protection*, 2011, pp. 1125-1129.

[2] S. Li, W. Chen, X. Yin, D. Chen and O. P. Malik, "Integrated Transverse Differential Protection Scheme for Double-Circuit Lines on the Same Tower," *IEEE Trans. Power Delivery*, vol. 33, no. 5, pp. 2161-2169, Oct. 2018.

[3] M. S. Jones, D. W. P. Thomas and C. Christopoulos, "A nonpilot phase selector based on superimposed components for protection of double circuit lines," *IEEE Trans. Power Delivery*, vol. 12, no. 4, pp. 1439-1444, Oct. 1997.

[4] J. Wijekoon, A. D. Rajapakse and N. M. Haleem, "Fast and Reliable Method for Identifying Fault Type and Faulted Phases Using Band Limited Transient Currents," *IEEE Trans. Power Delivery*, 2020.

[5] B. W. Jackson, M. Best and R. H. Bergen, "Application Of a Single Pole Protection Scheme to a Double-Circuit 230 kV Transmission Line," in *52nd Annual Georgia Tech Protective Relay Conference*, 1998, pp. 1-35

[6] V. H. S. Reyna, J. C. R. Velázquez, H. E. P. Félix, H. J. A. Ferrer, D. S. Escobedo and J. G. Guerrero, "Transmission Line Single-Pole Tripping : Field Experience in the Western Transmission Area of Mexico," in *37th Annual Western Protective Relay Conference*, 2010, pp. 1-12.

[7] A. Jamehbozorg and S. M. Shahrtash, "A decision tree-based method for fault classification in double-circuit transmission lines," *IEEE Trans. on Power Delivery*, vol. 25, no. 4, pp. 2184-2189, Oct. 2010.

[8] N. Kothari, B. R. Bhalja, V. Pandya, P. Tripathi and S. Jena, "A phasor-distance based faulty phase detection and fault classification technique for parallel transmission lines," *International Journal of Emerging Electric Power Systems*, vol. 21, no. 4, 2020.

[9] R. Abboud and D. Dolezilek, "Time-Domain Technology – Benefits to Protection, Control, and Monitoring of Power Systems," in *Int. Conf. and Exhibition – Relay Protection and Automation for Electric Power Systems*, Saint-Petersburg, 2017.

[10] A. Prasad, J. B. Edward and K. Ravi, "A review on fault classification methodologies in power transmission systems: Part—I," *Journal of Electrical Systems and Information Technology*, vol. 5, no. 1, pp. 48-60, May, 2018.

[11] A. Jain, . A. S. Thoke, E. Koley and R. N. Patel, "Fault classification and fault distance location of double circuit transmission lines for phase to phase faults using only one terminal data," in *2009 Int. Conf. on Power Systems*, Kharagpur, 2009, pp. 1-6.

[12] M. R. Noori and S. M. Shahrtash, "Combined Fault Detector and Faulted Phase Selector for Transmission Lines Based on Adaptive Cumulative Sum Method," *IEEE Trans. Power Delivery*, vol. 28, no. 3, pp. 1779-1787, July 2013.

[13] R. K. Aggarwal, Q. Y. Xuan, D. R. W., A. T. Johns and A. Bennett, "A novel fault classification technique for double-circuit lines based on a combined unsupervised/supervised neural network," *IEEE Trans. on Power Delivery*, vol. 14, no. 4, pp. 1250-1256, Oct. 1999.

[14] N. Saravanan and A. Rathinam, "A Comparitive Study on ANN Based Fault Location and Classification Technique for Double Circuit Transmission Line," in *2012 Fourth Int. Conf. on Computational Intelligence and Communication Networks*, Mathura, 2012, pp. 824-830

[15] E. Da Silva Oliveira, A. H. Anzai and W. A. Gaspar, "A high accuracy Fuzzy-Logic based fault classification in double-circuit transmission corridors," in *2014 11th IEEE/IAS Int. Conf. on Industry Applications*, Juiz de Fora, 2014, pp. 1-7.

[16] C. Cecati and K. Razi, "Fuzzy-logic-based high accurate fault classification of single and double-circuit power transmission lines," in *SPEEDAM 2012 - 21st Int. Symposium on Power Electronics, Electrical Drives, Automation and Motion*, Sorrento, 2012, pp. 883-889.

[17] A. A. Elbaset and T. Hiyama, "Fault detection and classification in transmission lines using ANFIS," *IEEJ Trans. on Industry Applications*, vol. 129, no. 7, pp. 705-713, 2009.

[18] A. Yadav and A. Swetapadma, "Improved first zone reach setting of artificial neural network-based directional relay for protection of double circuit transmission lines," *IET Generation, Transmission and Distribution*, vol. 8, no. 3, pp. 373-388, 2014.

[19] M. N. Haleem and A. D. Rajapakse, "A Transient Based Phase Selection Method for Transmission Line Protection," in *Int. Conf. on Power System Transients*, Perpignan, 2019.

[20] M. R. Noori and S. M. Shahrtash, "A novel faulted phase selector for double circuit transmission lines by employing adaptive cumulative sum-based method," in *012 11th Int. Conf. on Environment and Electrical Engineering*, Venice, 2012, pp. 365-370.

[21] N. M. Haleem and A. D. Rajapakse, "Fault-Type Discrimination in HVDC Transmission Lines Using Rate of Change of Local Currents," *IEEE Trans. on Power Delivery*, vol. 35, no. 1, pp. 117-129, February 2020.